Article

Development of an Exoskeleton-Type Assist Suit Utilizing Variable Stiffness Control Devices Based on Human Joint Characteristics †

Seigo Kimura [1,*] **, Ryuji Suzuki** [1] **, Katsuki Machida** [1] **, Masashi Kashima** [1] **, Manabu Okui** [1] **, Rie Nishihama** [2] **and Taro Nakamura** [1]

1   Department of Precision Mechanics, Faculty of Science and Engineering, Chuo University, 1-13-27 Kasuga, Bunkyo-ku, Tokyo 112-8551, Japan; ryu_suzuki@bio.mech.chuo-u.ac.jp (R.S.); k_machida@bio.mech.chuo-u.ac.jp (K.M.); m_kashima@bio.mech.chuo-u.ac.jp (M.K.); manabu.okui48@gmail.com (M.O.); nakamura@mech.chuo-u.ac.jp (T.N.)
2   Research and Development Initiative, Chuo University, 1-13-27 Kasuga, Bunkyo-ku, Tokyo 112-8551, Japan; r_nishihama@bio.mech.chuo-u.ac.jp
*   Correspondence: s_kimura@bio.mech.chuo-u.ac.jp
†   This paper is an extended version of the conference paper by Seigo Kimura; Ryuji Suzuki; Masashi Kashima; Manabu Okui; Rie Nishihama; and Taro Nakamura. Assistive method that controls joint stiffness and antagonized angle based on human joint stiffness characteristics and its application to an exoskeleton. In Proceedings of the 19th International Conference on Advanced Robotics (ICAR), Belo Horizonte, Brazil, 2–6 December 2019.

Abstract: In this paper, the prototype of the assistive suit for lower limbs was developed. The prototype was based on an assist method with joint stiffness and antagonized angle control. The assist method comprises a system consisting of a pneumatic artificial muscle and a pull spring, which changes the joint stiffness and the antagonized angle to correspond to the movement phase and aims at coordinated motion assistance with the wearer. First, the characteristics of the developed prototype were tested. It was confirmed that the measured value of the prototype followed the target value in the relationship between torque and angle. In addition, there was hysteresis in the measured value, but it did not affect the assist. Next, the evaluation of standing-up and gait assist by measuring electromyography (EMG) of the knee extensor muscle was conducted using the prototype. In all subjects, a decrease in EMG due to the assist was confirmed. In one subject, the maximum decrease rate at the peak of the EMG was about 50% for standing-up motion and about 75% for gait motion. From the results of these assist evaluations, the effectiveness of the assist method based on the joint stiffness and antagonistic angle control using the prototype was confirmed.

Keywords: assist suit; variable stiffness; artificial muscle; exoskeleton-type; walking assist; standing-up assist

1. Introduction

Elderly people experience muscle weakness as they age [1]. The degree of decline in the lower limbs is particularly high, and muscle weakness in the lower limbs interferes with daily activities, such as standing up and walking [2,3]. This leads to limitations in daily life activities, and a decrease in the quality of life [4,5]. Therefore, support for elderly independence and rehabilitation is required.

One of the solutions to these problems in muscle weakness is the usage of exoskeleton-type assist suits. These assist suits are used for various purposes, including power assistance, rehabilitation, and independence support [6–10]. Most of the existing assist suits are driven by a motor and a reducer to provide angle control [6,10,11]. These devices require soft movements to coordinate with the wearer. Therefore, the motor is controlled to reproduce the flexibility. However, that flexibility is limited by the performance of the

actuator and the controller. Therefore, it has insufficient flexibility in situations that require a fast response, such as collisions with a disturbed environment or misalignment between the suit and the wearer during the assist.

Some assist suits use pneumatic artificial muscles [7–9]. Due to high power density, artificial muscles must have a lightweight and flexible structure while achieving high assisting power. However, providing smooth assistance in accordance with the wearer's movements is difficult because the pressure applied to the artificial muscles is always constant.

We focus herein on the principle of human joint drive. Human beings operate with elastic muscles, and have structural flexibility in their joints. Furthermore, the antagonistic arrangement of the muscles across joints allows the control of angle, torque, and stiffness [12,13]. These structurally variable stiffness characteristics of human beings allow them to move with respect to disturbances caused by their structural flexibility. Therefore, we developed a variable elastic assist suit, called "Airsist I", using a pneumatic artificial muscle, which is a variable elastic element [9,14]. In a previous study, we proposed a control law that simulates human stiffness changes and confirmed the effectiveness of the assist by electromyography (EMG) and assisted torque.

In contrast, humans, as hardware, can take advantage of the variable stiffness property to simplify and increase the motion control performance [15,16]. For example, in the knee joint during steady walking, the joint torque is not finely controlled, and the joint stiffness is switched and driven during the stance and swing phase [17]. This is a control based on the human structure, structural flexibility of joints, and variable stiffness characteristics, which can simplify the control compared to building the same system with motor angle control, etc. Previous studies [9,14] focused only on structural flexibility and did not address control simplification.

In this study, we propose an assist method by controlling the joint stiffness ([N m/deg], in this paper, "deg" means the abbreviation of degree and is used as the unit of angle.) and the antagonized angle (angle when torque is 0 N m, [deg]) as variable elastic elements. The proposed system consists of a pneumatic artificial muscle and a pulling spring, and aims at coordinated motion assistance with the wearer by changing the joint stiffness and the antagonized angle to correspond to the phase of the motion.

In our previous research [18], a joint structure in which a pneumatic artificial muscle and a pull spring are antagonistically arranged (hereinafter referred to as a one-sided spring antagonized joint) and its mathematical model were proposed to realize this assist method, and the characteristics of the one-sided spring antagonized joint were investigated. It was found that the angle and torque of the one-sided spring antagonized joint are directly proportional to each other, and that the joint stiffness and the antagonized angle switch with the applied pressure. In order to investigate the changes in joint stiffness and antagonized angle during human motion, we analyzed the standing-up and gait motion. In the knee joint, standing-up and gait consisted of two motions, and the joint stiffness and antagonized angle were switched in each motion. The absolute values of the joint angle and the joint torque were directly proportional to each other in both the standing-up and gait motions, showing the same tendency as that of the one-sided spring antagonized joint. Therefore, it is considered that the one-sided spring antagonized joint can assist in standing-up and gait motion.

In this paper, an assist device is developed and evaluated based on the findings of the previous study [18]. The main contributions of this paper are as follows.

1. A prototype of an assistive suit for lower limbs based on the one-sided spring antagonized joint is developed. The prototype is tested to confirm that its behaviors are similar to the theoretical one-sided spring antagonized joint.
2. The effectiveness of the assist by controlling the stiffness and antagonized angle of the one-sided spring antagonized joint is confirmed. For this purpose, we perform evaluation experiments using the prototype to measure EMG in assisting standing-up and gait motions.

This paper is organized as follows: Section 2 describes the structure and characteristics of the one-sided spring antagonized joint and the assist method; Section 3 describes the prototype of the assistive suit for lower limbs and its characteristics; Section 4 describes the assist evaluation experiments for the standing-up and gait motion; and Section 5 concludes. The experiments on the human subjects described in this paper were approved by the Ethics Review Committee of Chuo University (No. 2017-27).

2. One-Sided Spring Antagonized Joint

2.1. Structure

We propose a joint structure, in which artificial muscles and elastic elements are antagonistic to each other as a configuration with structurally variable stiffness and antagonistic angle (Figure 1 [18–20]). The elastic element herein is a pull spring with a weight similar to that of the artificial muscle and does not require a new power source. This configuration allows for structure simplification and a much smaller and lighter pneumatic system compared to the use of two artificial muscles in a previous study [9].
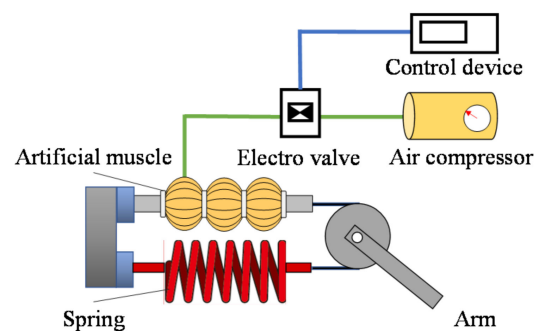

Figure 1. Schematic of one side spring antagonized joint [18–20].

2.2. Straight Fiber-Type Artificial Muscle

The shape of the artificial muscle used in this method is shown in Figure 2 [9]. This artificial muscle consisted of a cylindrical natural rubber tube and a carbon fiber enclosure. The carbon fibers were arranged in the axial direction of the rubber tube; hence, the rubber tube did not extend in the axial direction. When air pressure is applied, it expands only in the radial direction and contracts in the axial direction. As a result, the maximum contraction rate for this artificial muscle during no-load was as high as 38%, while that for the conventional McKibben-type artificial muscle was only 25% [21]. The contractile force at an applied pressure of 0.50 MPa was also high (2000 N) compared to 500 N for the McKibben-type artificial muscle [22]. A ring was placed between the artificial muscles. The ends of the rubber tube were secured with terminals. The ring was used to adjust the force and amount of contraction. The elastic modulus of this artificial muscle was structurally altered by applying air pressure. Variable elasticity was achieved [9].
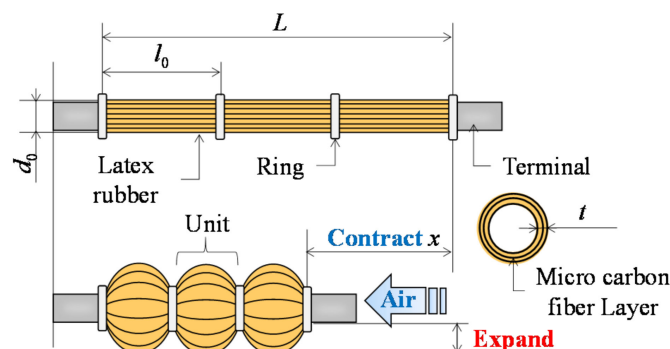

Figure 2. Straight-fiber-type artificial muscle [9].

2.3. Modeling

The model diagram of the one-sided spring antagonized joint is shown in Figure 3a [18–20]. Suffix 1 denotes a spring, while suffix 2 represents an artificial muscle. The displacements of the spring (x_1) and the artificial muscle (x_2) were determined by the pulley diameter r, target angle θ_d, and initial angle θ_a when the spring is of a natural length, and the artificial muscle is fully extended, as expressed in Equation (1).

$$x_1 = x_2 = r(\theta_\mathrm{d} - \theta_a) \tag{1}$$

(a) Model   **(b)** Feed-forward controller
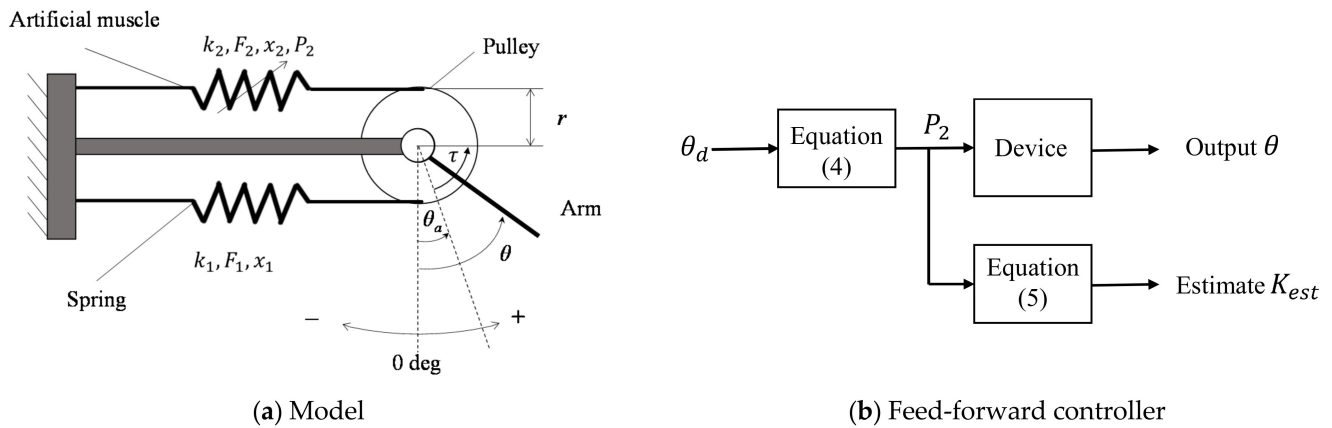
Figure 3. Model and block diagram of the one-sided spring antagonized joint [18–20].

The restoring force F_1 of the spring was determined by the displacement of the artificial muscle x_2 and the spring constant k. The contractile force F_2 of the artificial muscle was determined by the displacement x_2 of the artificial muscle and the applied pressure P_2 from a previous study, which is expressed by Equation (2) [23].

$$F_2(x_2, P_2) = (c_2 x_2 + d_2)P_2 + (f_2 x_2 + g_2) \tag{2}$$

Note that c_2, d_2, f_2, and g_2 are the coefficients obtained from a previous study [23]. Solving the balance of the moment around the center of the pulley gives the torque τ expressed by Equation (3).

$$\tau = (r^2 k_1 - r^2 c_2 P_2 - r^2 f_2)(\theta_\mathrm{d} - \theta_\mathrm{a}) - r d_2 P_2 - r g_2 \tag{3}$$

Solving for the applied pressure P_2 from Equation (3) gives Equation (4). The estimated joint stiffness K_{est} is the amount of change in torque with respect to the angular displacement; hence, it is expressed by Equation (5) from Equation (2).

$$P_2 = \{- \tau + r^2(k_1 - f_2)(\theta_\mathrm{d} - \theta_\mathrm{a}) - r g_2\} / \{ r^2 c_2(\theta_\mathrm{d} - \theta_\mathrm{a}) + rd\} \tag{4}$$

$$K_{est} = \Delta \tau / \Delta \theta = - r^2 c_2 P_2 + r^2 k_1 - r^2 f_2 \tag{5}$$

A feed-forward controller for torque $\tau = 0$ was constructed from Equations (4) and (5). Its outline is shown in Figure 3b [18–20]. First, the target angle θ_d was input into Equation (4) to obtain the required applied pressure P_2. The angle was then output by putting the calculated applied pressure P_2 into the one-sided spring antagonized joint. The joint stiffness can be calculated using Equation (5). The angle and the stiffness cannot be controlled independently, but can be designed to arbitrary values.

2.4. Characteristic

The relationship between the joint angle and the joint torque of a one-sided spring antagonized joint was calculated. The change in the joint stiffness and antagonized angle

was then investigated. The joint stiffness is a derivative of the joint torque by the joint angle. The antagonized angle is the joint angle when the joint torque is 0 N m.

Each parameter value of the one-sided spring antagonized joint when the knee joint was assumed to be assisted is presented in Table 1 [18–20]. How to determine the parameter values is discussed below. Coefficients c_2, d_2, f_2, and g_2 for determining the contractile force of the artificial muscles from a previous study were used [23]. The upper limit of the pressure P_2 applied to the artificial muscle was 0.39 MPa, because the artificial muscles worked stably up to 0.40 MPa empirically. The pulley diameter was 22.0×10^{-3} m, in accordance with the pulley diameter of the assist suit in the previous study [9]. Next, we considered the spring constant k_1. The joint range of motion for standing up and walking was approximately 0–90 deg. Therefore, when the torque $\tau = 0$ N m and the initial angle $\theta_a = 0$ deg, the driving range of the joint was assumed to be from 0 to 90 deg. According to Equation (3), to achieve a joint angle $\theta_d = 90$ deg at the applied pressure $P_2 = 0.3$ MPa, the spring constant k_1 should be less than 5000 N/m. Therefore, the spring constant k_1 was determined as 4900 N/m herein.

Table 1. Parameter values of the one-sided spring antagonized joint [18–20].

c_2	-67.5×10^{-3}	r	22.0×10^{-3} [m]
d_2	3.60×10^{-3}	θ_a	0 [deg]
f_2	1.81×10^3	P_2	0 ~ 0.39 [MPa]
g_2	273	k_1	4900 [N/m]

The relationship between the calculated joint angle and the joint torque of the one-sided spring antagonized joint is shown in Figure 4 [18–20]. The joint stiffness and antagonized angle values for each applied pressure are presented in Table 2 [18–20]. The joint torque τ' of the vertical axis was set to $\tau' = -\tau$. The joint angle θ' of the horizontal axis was set to $\theta' = 90 - (\theta_d - \theta_a)$ to match the joint angle definition in the later motion analysis. Figure 4 shows that the angle and the absolute value of the torque were positively proportional. When the applied pressure changed, the antagonized angle changed along with the joint stiffness (slope of the graph). This result indicates that the antagonized angle and the joint stiffness of the one-sided spring antagonistic joint can be controlled by controlling the applied pressure.
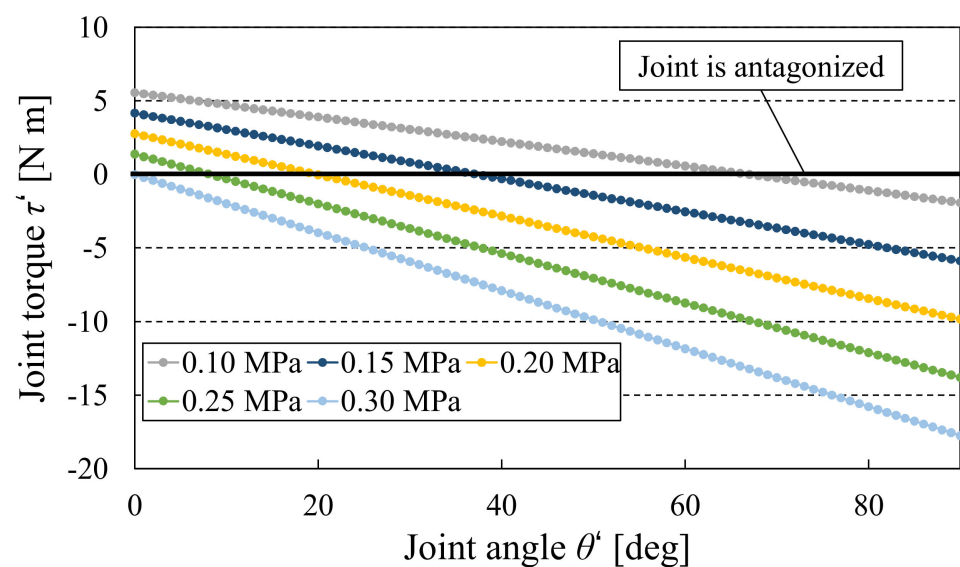
Figure 4. Relationship between the joint torque and the joint angle of the one-sided spring antagonized joint [18–20].

Table 2. Stiffness and antagonized angle of the one-sided spring antagonized joint [18–20].

Applied Pressure [MPa]	Stiffness [N m/deg]	Antagonized Angle [deg]
0.10	0.0831	67.0
0.15	0.112	37.4
0.20	0.140	19.8
0.25	0.169	8.2
0.30	0.197	0.0

2.5. Assistive Method

The active assist image of the one-sided spring antagonized joint is shown in Figure 5 [18]. Air pressure was applied such that the antagonized angle θ_d of the one-sided spring antagonized joint was larger than the human joint angle θ_1. The one-sided spring antagonized joint generated torque τ_{device}, which is the product of the stiffness K_{device} and the angle presented by the one-sided spring antagonized joint, in the range of the human joint angle θ_1 and the antagonized angle θ_d of the one-sided spring antagonized joint. The torque was in the same direction as the human movement. The one-sided spring antagonized joint had an active assist to the human joint.
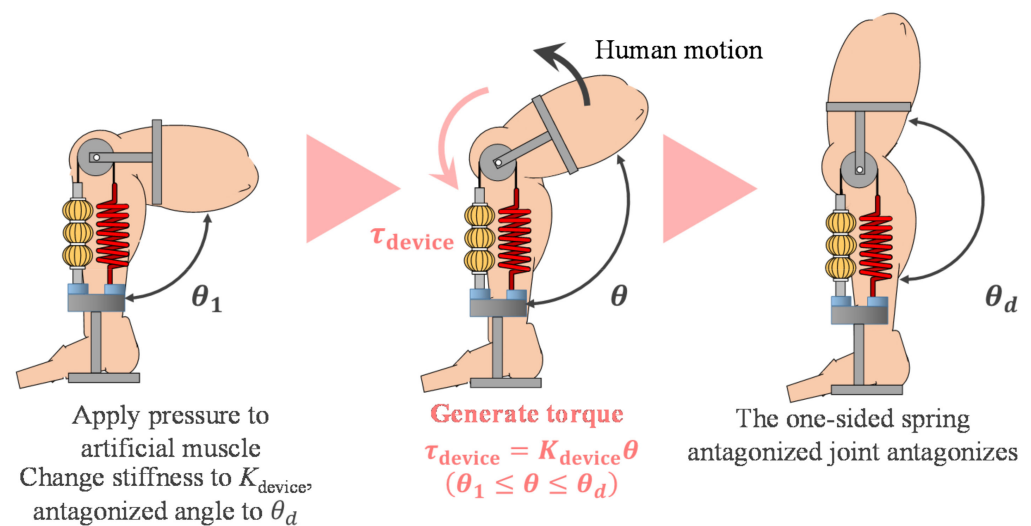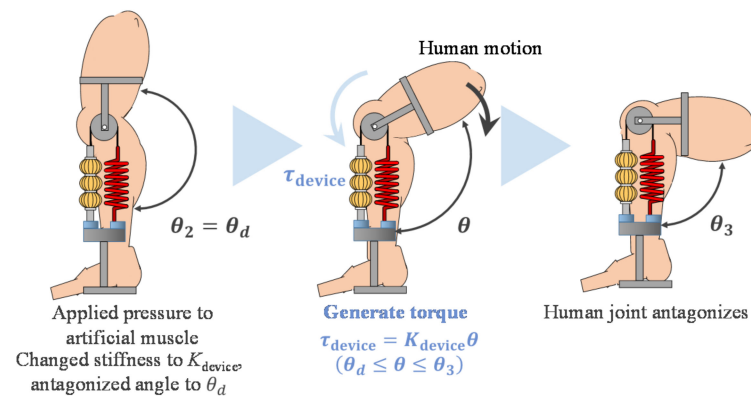

Figure 5. Activity assisted by the one-sided spring antagonized joint [18]. © IEEE 2019.

Figure 6 [18] shows the image of a passive assist. Air pressure was applied such that the antagonized angle θ_d of the one-sided spring antagonized joint and the human joint angle θ_2 were the same. The one-sided spring antagonized joint generated torque τ_{device}, which was the product of the stiffness K_{device} and the angle presented by the one-sided spring antagonized joint, in the range of the human joint angle θ_3 and the antagonized angle θ_d of the one-sided spring antagonized joint. Its torque was opposed to human movement and supported the human's own weight. In other words, the one-sided spring antagonized joint had a passive assist to the human joint.

To realize such an assist, the joint angle and the absolute value of the joint torque must be positively proportional to each other, as in the case of the one-sided spring antagonized joint in Figure 4.

Figure 6. Passive assisted by the one-sided spring antagonized joint [18]. © IEEE 2019.

3. Prototype

3.1. Structure

Figure 7 [20] depicts the CAD model of the prototype (one unit and a configuration for knee assist) and the appearance of the produced prototype. Each unit consisted of a straight fiber-type artificial muscle, a spring, a rotary encoder (MES-6-500-PC, MICROTECH LABORATORY Inc.), a pneumatic valve (EXA-C6-02C3, CKD Co.), and a pressure sensor (SEU11-6UA, NIHON PISCO Co.). Each unit measured 380 mm long and 100 mm wide and weighed 2.4 kg. When configured for knee assist as shown in Figure 7c,d, the length and the width were 580–780 mm and 100 mm, respectively, and the weight was 3.1 kg. Figure 7a,b depict that the artificial muscle and the spring were antagonistically arranged similar to the model of the one-sided spring antagonized joint shown in Figure 3a. The force of the artificial muscle and the spring was transmitted to the pulley by the timing belt to generate torque. Table 1 shows each parameter value.

3.2. Characteristic Test

3.2.1. Purpose

The produced prototype (Figure 7) showed the theoretical properties of a one-sided spring antagonized joint (Figure 4). In this experiment, the joint torque and the joint angle of the prototype were measured for each applied pressure.

3.2.2. Experimental Environment

Figure 8 [20] shows the experimental environment. The prototype was fixed and driven in a vise. A proportional solenoid valve (ITV2050-312L, SMC Co., Tokyo, Japan) was controlled by a commanded signal from MATLAB/Simulink and ControlDesk (dSPACE Co., Tokyo, Japan) through a D/A converter to supply the applied pressure to the artificial muscles. A compressor was used as the air pressure source. The angle and the external force were measured by a digital force gauge (FGP-50, NIDEC-SHIMPO Co., Tokyo, Japan) hooked to the tip of the prototype.

3.2.3. Experimental Method

The experiments were performed from a position where the joint angle was 90 deg. The command pressures to the artificial muscles were set at 0.10, 0.20, and 0.30 MPa. The joint angles of each applied pressure were measured when the joint became antagonistic. The external force for each applied pressure was measured by a force gauge. The external force was measured in increments of 10 deg in the direction of the decreasing angle from the antagonistic position. Once the timing belt began to sag, the joint torque exceeded 20 N m, or the range of motion of the joint was reached (0–90 deg), the angle was measured in increments of 10 deg in the direction of the increasing angle. The joint torque was calculated from the measured external force and the length of the unit (0.40 m).
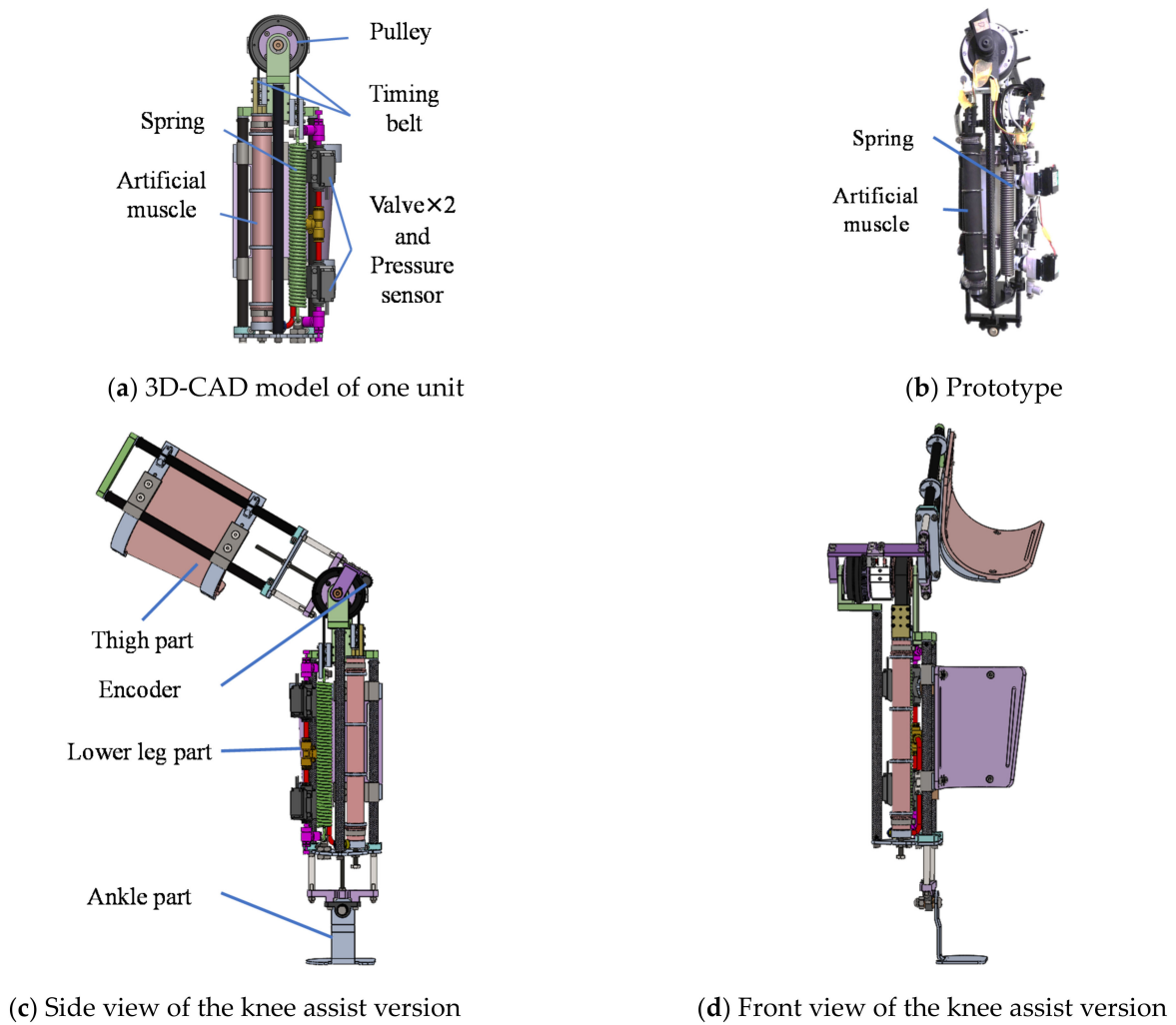
(**a**) 3D-CAD model of one unit

(**b**) Prototype

(**c**) Side view of the knee assist version

(**d**) Front view of the knee assist version

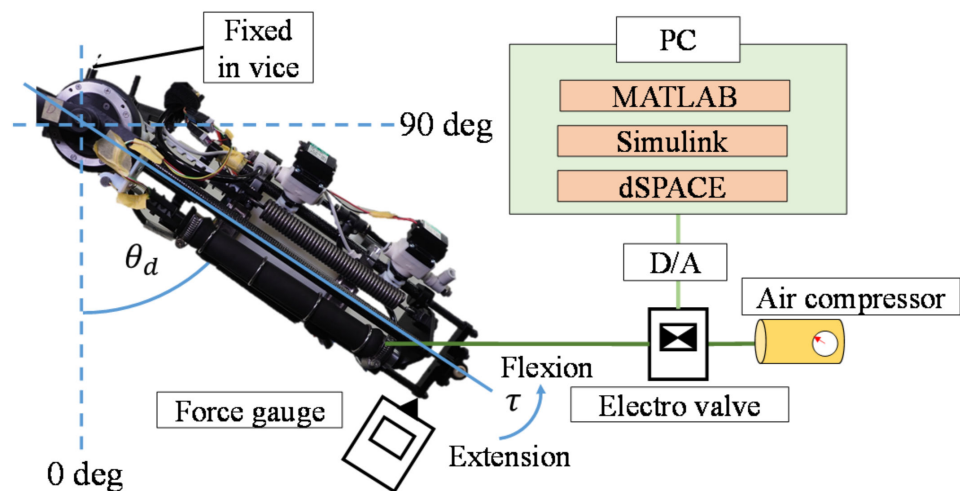**Figure 7.** Prototype of the one-sided spring antagonized joint [20].

**Figure 8.** Experimental environment of basic characteristics [20].

3.2.4. Result and Discussion

Figure 9 [20] depicts the relationship between the torque and the angle for each applied pressure, which shows that the absolute value of the torque increased with the increase of the angle or decreased with the decrease of the angle. In addition, the stiffness and the

antagonized angle changed with the applied pressure. These results confirmed that the produced prototype behaved similarly to the theoretical one-sided spring antagonized joint. However, the measured values had hysteresis, which is thought to be caused by the friction in the pulley section, and hysteresis of the pneumatic artificial muscles. The hysteresis of the measured values can also be confirmed in the characteristic test of the previous study (joint structure with two artificial muscles antagonistically arranged) [14]. The assist effect in that previous study [14] was confirmed in a later assist experiment. Therefore, the hysteresis of this experiment was thought to also have no effect on the later assist evaluation.
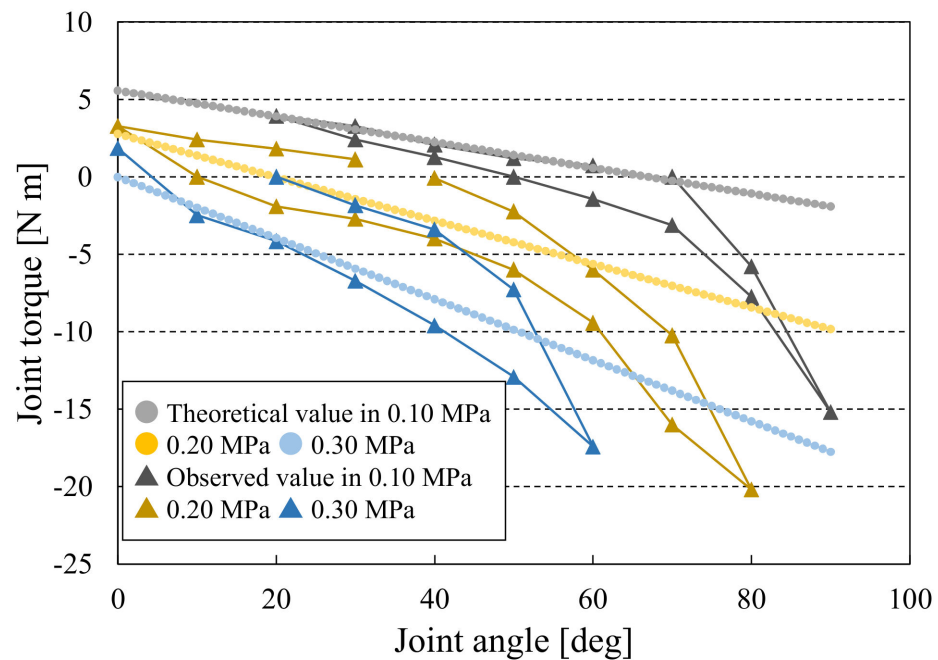
Figure 9. Relationship between the joint torque and the joint angle of theoretical and observed values [20].

4. Assist Evaluation

4.1. Purpose

In this experiment, a prototype was used to assist a person in the standing-up motion and gait motion. The effectiveness of the assist by the stiffness and the antagonized angle control in the one-sided spring antagonized joint was confirmed by EMG. The prototype performed assistance of the knee joint when standing up from a sitting position and during gait motion.

4.2. Assist of Standing-up Motion

4.2.1. Subjects

The subjects were three healthy males. Table 3 presents their detailed information. The subjects were briefed beforehand on the purpose and methods of the experiment. They consented to participate in this experiment.

Table 3. Subject information in the assist evaluation of the standing-up motion.

Subject	A	B	C
Age	22	24	22
Height [m]	1.80	1.75	1.74
Weight [kg]	90	70	54

4.2.2. Experimental Environment

Figure 10 depicts the experimental environment. Force plates (TF-4060-D, Tec Gihan Co., Tokyo, Japan, sampling Hz: 1000 Hz) and EMG sensors (Trigno Wireless EMG, DELSYS Co., Tokyo, Japan, Sampling rate: 2000 Hz) were used to measure the muscle potential. One force plate was placed under each foot of the subject, and the other was placed on the chair. The height of the chair, including the force plate, was set such that the joint angle of the knee was 90 deg when the subject was sitting with their buttocks in contact with the force plate on the chair.
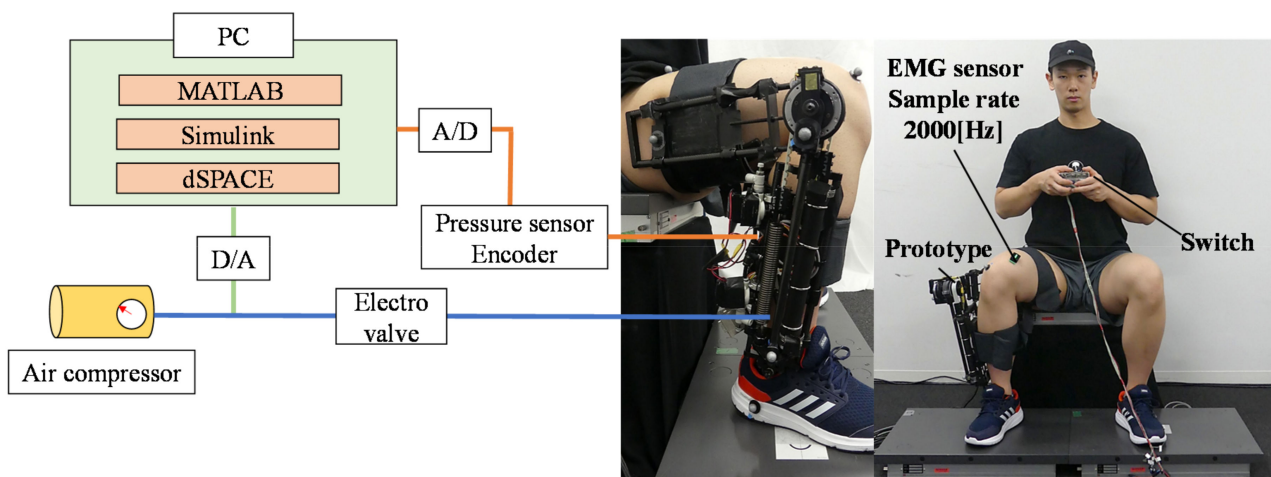
Figure 10. Experimental environment in the assist evaluation of the standing-up motion.

Subjects wore a prototype configured for knee assist on their right leg and had a switch in their hand to control the prototype. They were also seated on a chair containing a force plate. An EMG sensor was attached to the subject's vastus medialis muscle (knee extensor [24], vastus medialis muscle: VM). The force plates were used to monitor the subjects' ability to stand up with equal weight on their left and right legs. A compressor was used as the air pressure source for the prototype artificial muscles.

4.2.3. Assist Target Values

The assist target values for the device (assist suit) during the operation were determined from the joint stiffness and the antagonized angle obtained in motion analysis [18]. The applied pressure to the one-sided spring antagonized joint was then calculated. The joint stiffness in the assist target values was calculated by multiplying the joint stiffness average of each subject obtained from the motion analysis by the assist rate. The target antagonized angles used were the average of the results of the motion analysis for each subject. From the motion analysis, the standing-up motion is divided into the slouching phase, in which the buttocks are on the sitting surface, and the standing phase, in which the buttocks are off the sitting surface. The assist rates for the knee joint herein were 10% and 30% during the slouching and standing phases, respectively. Table 4 shows the assist target values for the standing-up motion calculated from these assist rates. In addition, the pressure applied to the one-sided spring antagonized joint was investigated based on the relationship between the applied pressure and the theoretical joint stiffness and antagonized angle in Table 2. The antagonized angles of the assist target value and the theoretical antagonized angles of the one-sided spring antagonized at each applied pressure (0.05 MPa increments, range: 0.00–0.30 MPa) were compared in this study. The applied pressure with the greatest theoretical joint stiffness within ±15 deg of the target antagonized angle (exceptionally within ± 25 deg in the slouching phase) was adopted. Therefore, the applied pressures at the knee joint were set to 0.10 MPa and 0.30 MPa in the slouching and standing phases, respectively.

Table 4. Assist target values in the standing-up motion.

Assist Motion	Standing-up Motion	
Phase **Assist Type**	**Slouching** **Passive**	**Standing** **Active**
Criteria for joint stiffness [N m/deg]	11.1	0.625
Criteria for antagonized angle [deg]	92	4.73
Assist rate [%]	10	30
Target joint stiffness [N m/deg]	1.11	0.188
Target antagonized angle [deg]	92	4.73
Applied pressure [MPa]	0.10	0.30
Joint stiffness of the device [N m/deg]	0.0831	0.197
Antagonized angle of the device [deg]	67	0

4.2.4. Operation Method

The assist pattern and the applied pressure in the prototype were sitting (0.0 MPa), slouching (0.10 MPa), standing (0.30 MPa), and standing straight (0.39 MPa). In Section 4.2.3, the only assist patterns were in the slouching and standing phases. We added the assist patterns in the sitting on a chair and standing straight phases in the present experiment because performing the sitting on a chair and standing straight postures is necessary before and after the standing motion. Figure 11 shows the prototype operation. In this experiment, the subjects switched the assist pattern according to the timing of their confidence movements. They can also switch the assist (pressure applied to the artificial muscles) in the order of sitting, slouching, standing, and standing straight with each pressing of one switch.
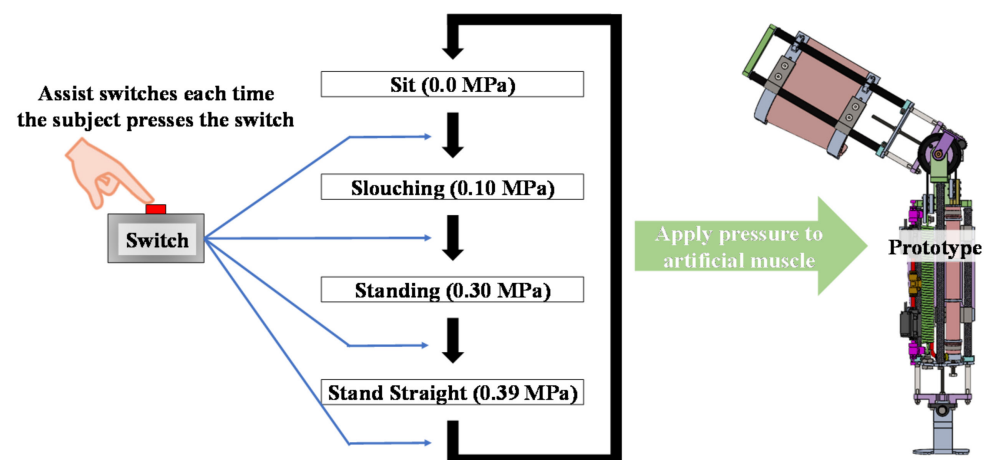
Figure 11. How to switch the assist mode with a switch.

4.2.5. Experimental Method

The experiment on the standing-up motion was performed in two states: With and without the prototype. First, the experiment was started with the prototype attached. The subjects were instructed to stand up naturally for approximately 2 s from sitting on a chair. They were then instructed to use a switch to switch the assist according to their own posture.

After all trials with the prototype were completed, the prototype was removed from the subjects, and they stood up without the prototype. The subjects were then instructed to stand up naturally for approximately 2 s from the sitting on the chair position, which is similar to the instructions when the prototype was attached. Each experiment was started after sufficient practice. Each number of trials was five.

4.2.6. Analysis Method

The period from the beginning of the subject's movement to the end of the movement was defined as one standing-up cycle. The signal for one standing-up cycle obtained from the EMG sensor was used as an experimental result. The signal was also band-pass filtered (20–450 Hz) and full-wave rectified. After rectification, it was low-pass filtered (10 Hz). MATLAB 2019 was used for a series of computational processes.

4.2.7. Result and Discussion

Figure 12 shows the relationship between the EMG with and without assistance, and the relationship between the command and measured pressures for each subject. The experiment results show the average of five trials. The force plate confirmed that the subjects were standing up with their weight evenly distributed on left and right legs.

Figure 12a,c confirmed that the EMG in Subjects A and C decreased with assistance during the latter half of the slouching phase (period 40–50%). However, as shown in Figure 12b, the EMG in Subject B was increased in the assisted condition compared to the un-assisted condition.

This result has two reasons. First, Subject B was slow to switch from the sitting position to the slouching assist in response to the rise of EMG at approximately 40% of the cycle (Figure 12b). Therefore, Subject B was considered to have experienced the difference between the assisted movement and his own movement. Second, the rise of the measured pressure of Subject B was slower than that of Subjects A and C at approximately 40% of the period from the relationship of the applied pressure in Figure 12a–c, because the posture of Subject B at that time put load on the artificial muscles.
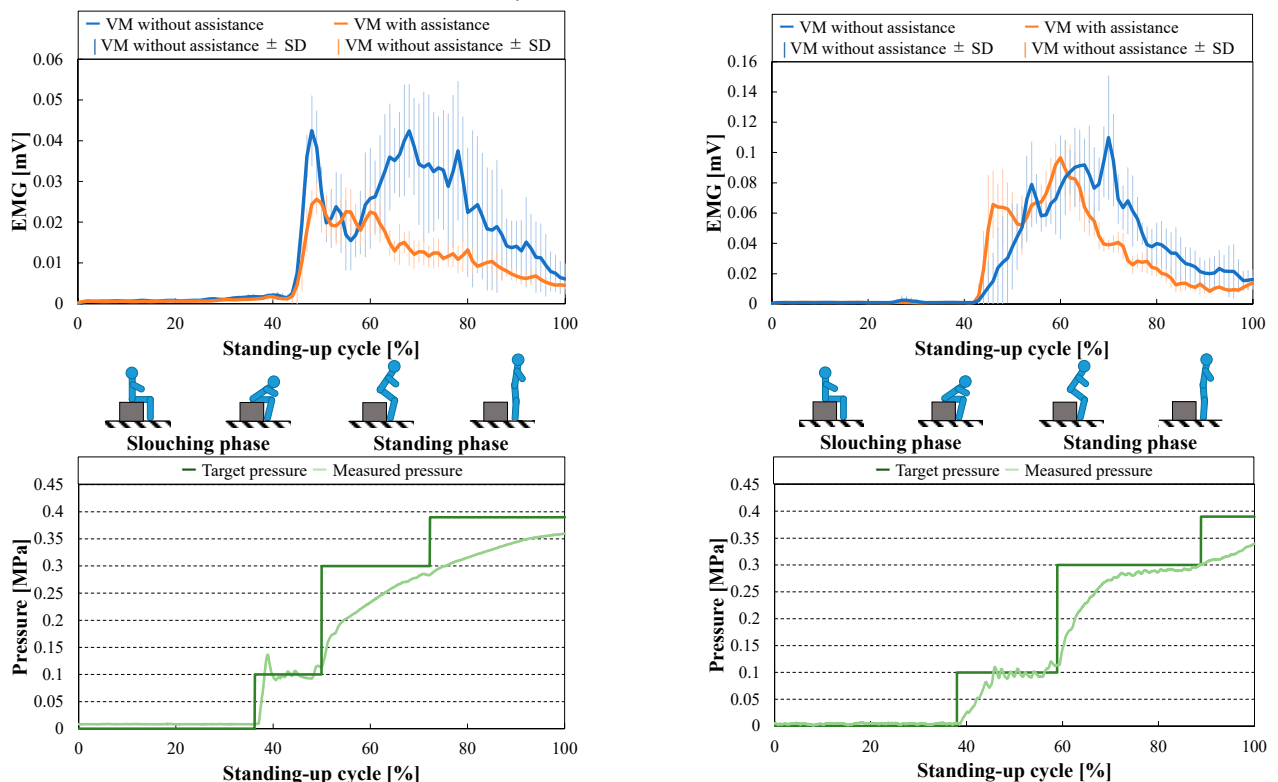
(**a**) VM (vastus medialis muscle) of electromyography (EMG) and applied pressure in Subject A.

(**b**) VM of EMG and applied pressure in Subject B.

Figure 11. *Cont.*
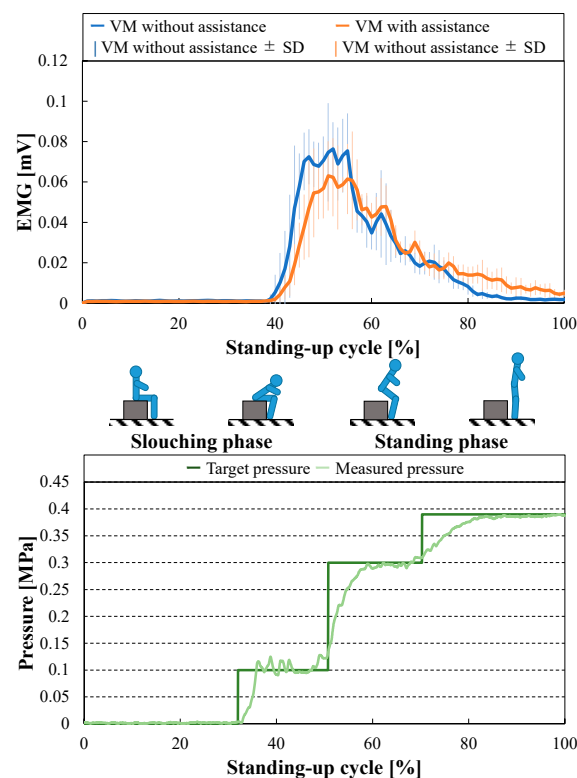
(**c**) VM of EMG and applied pressure in Subject C.

Figure 12. Comparison of EMG with and without assistance and applied pressure to the prototype in one standing-up cycle.

Figure 12 confirms that the assisted decrease in EMG was observed in Subjects A and B during the standing phase (cycle 50–100%). However, in Subject C, the EMG with assistance was increased more than those without assistance because the artificial muscles were quickly filled with pressure when switching from standing assist to standing straight assist (approximately 80% of the cycle) (Figure 12c). This result can be attributed to the low load on the artificial muscles caused by the posture of Subject C. As a result, Subject C was unable to match his own movement with the assisted movement, and the EMG with the assistance increased.

In conclusion, the effect of the standing-up assist using prototype was effective, confirming the effectiveness of the standing-up assist by the stiffness and the antagonized angle control in the one-sided spring antagonized joint. However, the effect of the assist was influenced by the timing of the assist, wearer's posture, and load on the artificial muscles. If the abovementioned conditions are met, as in Subject A, then the entire standing-up motion can be assisted.

4.3. Assist of Gait Motion

4.3.1. Subjects

The subjects were three healthy males. Table 5 presents their detailed information. The subjects were briefed beforehand on the purpose and methods of the experiment. They consented to participate in this experiment.

Table 5. Subject information in the assist evaluation of the gait motion.

Subject	D	E	F
Age	23	22	23
Height [m]	1.74	1.75	1.8
Weight [kg]	54	64	80

4.3.2. Experimental Environment

Figure 13 depicts the experimental environment. The EMG sensors and a motion capture system similar to Section 4.2.2 were used for EMG measurements. The subject attached the same prototype to his right foot as in Section 4.2 and held a switch in his hand. The switch was used to synchronize the data of the motion capture system and Control Desk in the gait assist. The subjects also walked on a treadmill, and EMG sensors were attached to the subjects' medial vastus muscles.
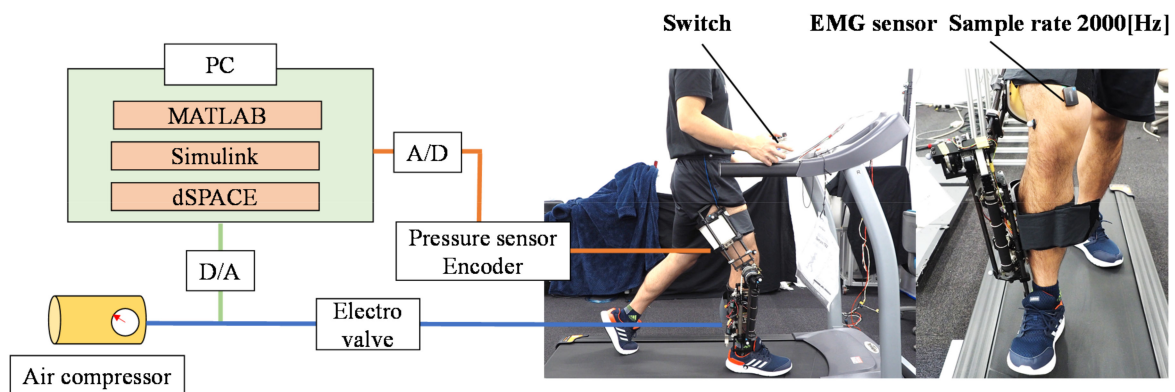

Figure 13. Experimental environment in assist evaluation of the gait motion.

4.3.3. Assist Target Values

As in Section 4.2.3, the assist target values and the pressure applied to the one-sided spring antagonist joint were investigated from motion analysis [18]. The gait motion is divided into the stance phase, when the feet are on the ground, and the walking phase, when the feet are off the ground. The assist rates for the knee joint were 10% and 30% during the standing and swing phases, respectively. Table 6 shows the assist target values for the gait motion calculated from these assist rates. The pressure applied to the one-sided spring antagonist joint was examined from Table 2. The applied pressure at the knee joint was set to 0.30 MPa during the standing phase and 0.10 MPa during the swing phase.

Table 6. Assist target values in the gait motion.

Assist Motion	Gait Motion	
Phase	Stance	Swing
Assist Type	Passive	Active
Criteria for joint stiffness [N m/deg]	3.86	0.329
Criteria for antagonized angle [deg]	13.4	63.2
Assist rate [%]	10	30
Target joint stiffness [N m/deg]	0.386	0.0987
Target antagonized angle [deg]	13.4	63.2
Applied pressure [MPa]	0.30	0.10
Joint stiffness of the device [N m/deg]	0.197	0.0831
Antagonized angle of the device [deg]	0	67

4.3.4. Operation Method

The assist pattern and applied pressure were set for the stance phase (0.30 MPa) and swing phase (0.10 MPa) from Section 4.3.3. In this experiment, the assist pattern was automatically switched at a predetermined time. The prototype moves cyclically from stance phase to swing phase to stance phase, and the subject is assisted by matching the movement. In addition, one gait cycle was defined as "from the time that the heel touches the ground to the time that the heel of the same foot touches the ground", and the cycle time was set to 1.5 s (0.90 s for the stance phase, and 0.60 s for the swing phase).

Switching the ideal assist pattern and the subject's movement is shown in Figure 14 as an image diagram using the relationship between the command pressure to the device and the angle of the knee joint during gait motion. The subject and the device reach a period of 0% at a command pressure of 0.30 MPa. They then reach a command pressure of 0.10 MPa around 40% of the cycle when knee extension is at maximum. In addition, they then reach a command pressure of 0.30 MPa at around 80% of maximum knee flexion.
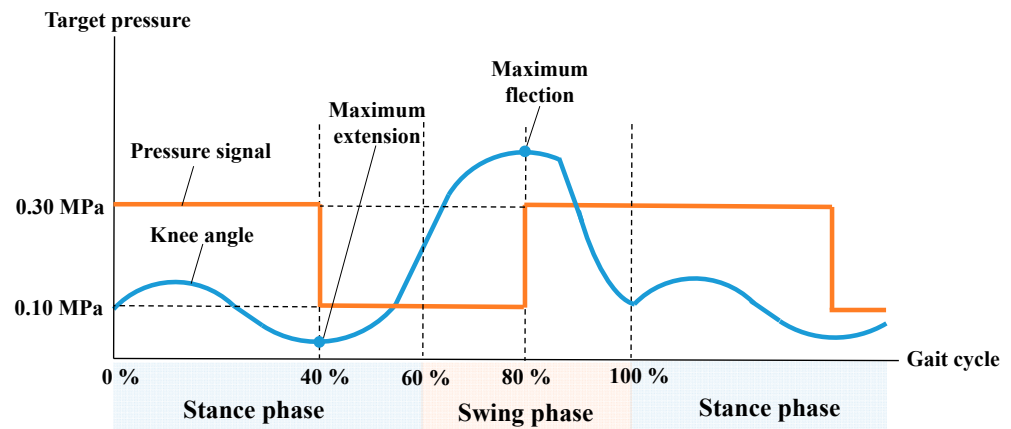
Figure 14. Image of the relationship between the target pressure on the device and the knee joint angle during gait motion. It represents the ideal assist pattern switching and subject movement.

4.3.5. Experimental Method

In the experiment, the subjects performed two gait motions, with and without the device. First, the experiment was started with the device attached. When the subject stands on a stationary treadmill, send a signal to the device to activate it for walking assistance. The subject steps in place as the device works. The subject operates the treadmill after checking that his movements and those of the device are in motion. When stopping the assist, stop the treadmill and step on the spot. Then, stop the signal of the walk assist and stop the operation of the device.

After all trials with the device were completed, the device was removed from the subject and the subject walked without the device. Subjects walked on a treadmill set to the same walking speed as when they were attached to the device. The treadmill's walking speed setting is 1.5 km/h. Each experiment was started after sufficient practice, and the number of trials was eight, with each trial lasting more than ten gait cycles. The method of analysis is the same as in Section 4.2.6, and the data of five gait cycles were adopted.

### 4.3.6. Result and Discussion

Figure 15 shows the relationship between the EMG with and without assistance, and the relationship between the actual and ideal pressure timing for each subject. Note that these experimental results are the average of five gait cycles. In the first half of the stance phase (around 0–20% of the cycle), it can be seen from Figure 15b,c that in subjects E and F, there was a decrease in EMG with assistance. However, as shown in Figure 15a, subject D has a higher muscle potential with assistance than without assistance. The reason for this is the change in muscle activity with walking speed. In the existing study [25], with treadmill walking at 4.8 km/h, the VM tends to be more active during the first half of the stance phase. This area is also affected by the walking speed, and the higher the walking speed, the higher the myoelectricity is [26]. In subject D, the walking speed of 1.5 km/h was slower and the muscle activity of the VM was smaller than in the existing study [25] (In Appendix A, the effect of walking speed on gait assist was examined). In addition, from Figure 15, it can be seen that the change in EMG with and without assistance is smaller in the swing phase than in the stance phase. This is because the VM tends to be less active during the swing phase of the gait motion, and the device does not inhibit the swing phase.
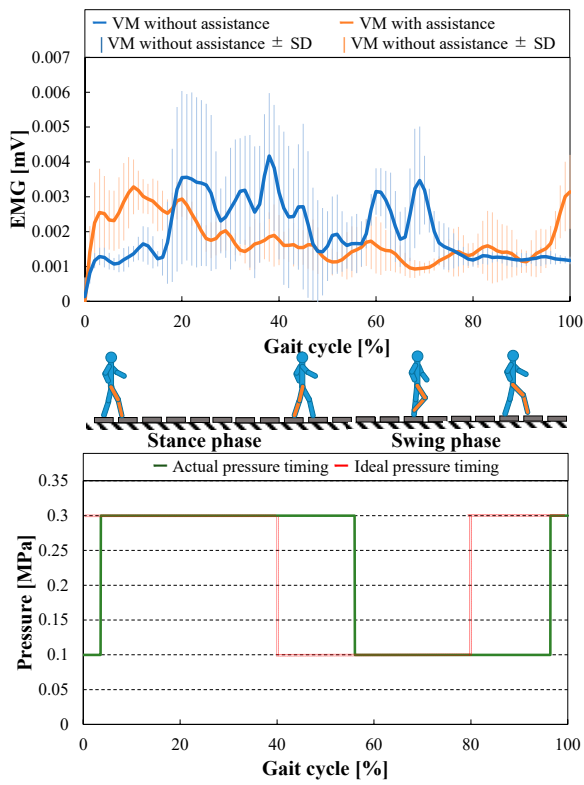
(**a**) VM of EMG and applied pressure in Subject D.
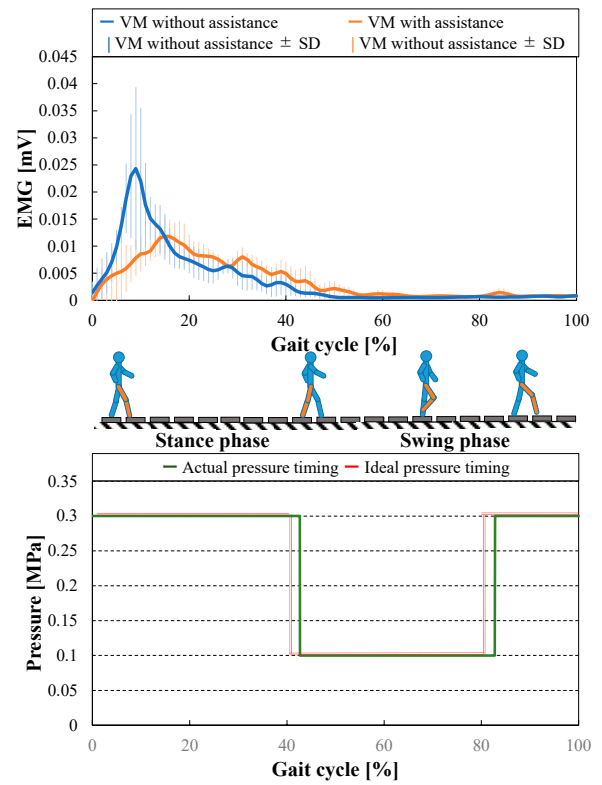
(**b**) VM of EMG and applied pressure in Subject E.
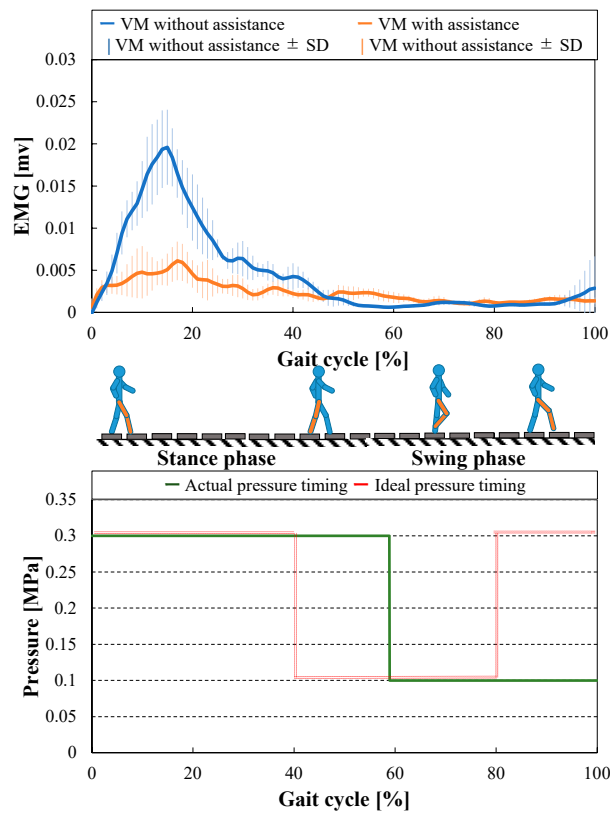
(**c**) VM of EMG and applied pressure in Subject F.

Figure 15. Comparison of EMG with and without assistance and applied pressure to the prototype in one gait cycle (1.5 km/h).

It can be seen from the pressure timing in Figures 14 and 15 that there is a difference between the idea pressure timing and the actual pressure timing in each subject, but this difference does not have an adverse effect (large increase in EMG). This is due to the low muscle activity of the VM in the differential area and the structural flexibility of the device to absorb the differences in movement between the device and the subject. In conclusion, the effect of the gait assist using prototype was effective, confirming the effectiveness of the standing-up assist by the stiffness and the antagonized angle control in the one-sided spring antagonized joint.

4.4. Summary of Assist Evaluation

In the Section 4, the assistive effects of the proposal method on the standing-up and gait motions were evaluated using the developed prototype. The assists targeted the knee joint and measured the VM, which is an extensor muscle of the knee. In the standing up from a sitting position, the EMG of the VM decreased by the assist, confirming the effectiveness of the standing- up assist with the prototype. However, it was found that the effectiveness of the assistance was affected by the load on the artificial muscles due to posture and the timing of the assistance.

In the gait motion (walking speed of 1.5 km/h), the EMG was decreased by the assistance during the stance phase, confirming the effectiveness of the gait assist. There was a difference between the ideal pressure timing and the actual pressure timing, but there was no adverse effect on the gait assist. This is because the muscle activity of the VM in the difference area was small and the structural flexibility of the device absorbed the difference in movement between the device and the subject. In conclusion, the effectiveness of the assist was confirmed by the stiffness and the antagonized angle control in the one-sided spring antagonized joint with the prototype.

5. Conclusions

The prototype of an assistive suit for lower limbs based on the one-sided spring antagonized joint was developed. The developed prototype showed the same behavior as the theoretical one-sided spring antagonized joint, since the absolute value of torque and angle were directly proportional, and the joint stiffness and antagonized angle changed depending on the applied pressure. Therefore, for this device to be able to assist effectively, the following conditions must be met: (1) The absolute value of the torque and the angle must be directly proportional, and (2) both the stiffness and the antagonistic angle must be switched by the motion. The prototype was designed to have a maximum output torque of 20 N m at a joint angle of 90 deg with an applied pressure of 0.30 MPa, but experimental data showed that the output torque was close to 20 N m even under other conditions due to hysteresis and friction. This would have a positive effect on the assist, since it implies a larger assist force. The prototype was used to evaluate the effect of the proposed method on assisting the knee joint during the standing-up motion and gait motion by using EMG. The experiment targeted the vastus medialis muscle (VM), which extends the knee, and performed knee assist in the standing-up motion. The results of standing-up assist showed that the assist decreased the EMG of the VM, confirming the effectiveness of the prototype assist in the standing-up motion. However, the effect of the assist was also affected by the timing of the assist and the load on the artificial muscle. Additionally, the results of gait assist (walking speed 1.5 km/h) showed that the assist decreased the EMG of the VM, confirming the effectiveness of the prototype assist in the gait motion. However, it can be seen that the change in EMG with and without assistance is smaller in the swing phase than in the stance phase. This is because the VM tends to be less active during the swing phase of the gait motion, and the device does not inhibit the swing phase. In conclusion, the effectiveness of the assist was confirmed by the stiffness and the antagonized angle control in the one-sided spring antagonized joint with the prototype.

In the future, since the parameters of the prototype and the assist rate for each movement were tentatively determined in this paper, an appropriate selection method will

be established with the opinions of the subjects in this experiment. The start, end, and switching of the assist in this experiment was done using a switch or a periodic switching method. We have succeeded in developing a motion judgment algorithm using the joint angle of the device for switching the assist [27], and we will conduct an assist evaluation experiment using this algorithm. The prototype will not only assist the knee joint, but also assists the hip joint, which assists the entire lower limb. Accordingly, the device is improved to be able to assist the entire lower limb.

Author Contributions: Conceptualization, S.K., T.N., and M.O.; methodology, S.K.; software, M.O.; validation, S.K., R.N., R.S., M.K., and K.M.; formal analysis, S.K.; investigation, S.K.; resources, S.K. and M.O.; data curation, S.K.; writing—Original draft preparation, S.K.; writing—Review and editing, M.O., R.N., and T.N.; visualization, S.K.; supervision, T.N.; project administration, T.N.; funding acquisition, T.N. All authors have read and agreed to the published version of the manuscript.

Institutional Review Board Statement: This study was approved by the Ethical Review for Research Involving Human Subjects, Faculty of Science and Engineering, Chuo University (No. 2017-27).

Informed Consent Statement: The purpose and methods of the experiment were explained to all subjects involved in this experiment, and their consent to participate in the experiment was obtained.

Data Availability Statement: The copyright permissions for [9,18] are given below. For [19,20], it was not necessary to apply for copyright permission because I am the author (JSME).

Conflicts of Interest: The authors declare no conflict of interest. The funders had no role in the design of the study; in the collection, analyses, or interpretation of data; in the writing of the manuscript, or in the decision to publish the results.

Appendix A.

Appendix A.1. Effect of the Walking Speed

Appendix A.1.1. Experimental Information

In this experiment, it is confirmed whether the assisting effect is obtained at faster walking speeds (3.0 km/h and 4.5 km/h) than the 1.5 km/h of Section 4.3. The subject is a single subject F in Section 4.3.1, and the experimental environment, operation, and experimental method are the same as in Section 4.3, except for the gait cycle time. The cycle time was set to 1.4 s (0.84 s for stance phase, and 0.56 s for swing phase) at a walking speed of 3.0 km/h, and 1.1 s (0.66 s for stance phase, and 0.44 s for swing phase) at a walking speed of 4.5 km/h.

Appendix A.1.2. Result and Discussion

Figure A1 shows the relationship between the EMG with and without assistance, and the relationship between the actual and ideal pressure timing for subject F. From Figure A1, it can be seen that there is a decrease in EMG due to the assistance in 0–20% of the cycle, the same as in Section 4.3. The pressure timing from Figures 14 and A1 shows that there is a difference in the actual pressure timing at walking speed of 3.0 km/h compared to the ideal pressure timing. However, due to the structural flexibility of the device, no negative effects of this difference are found. These results confirmed the effectiveness of the gait assist even at a walking speed of 3.0 km/h and 4.5 km/h.
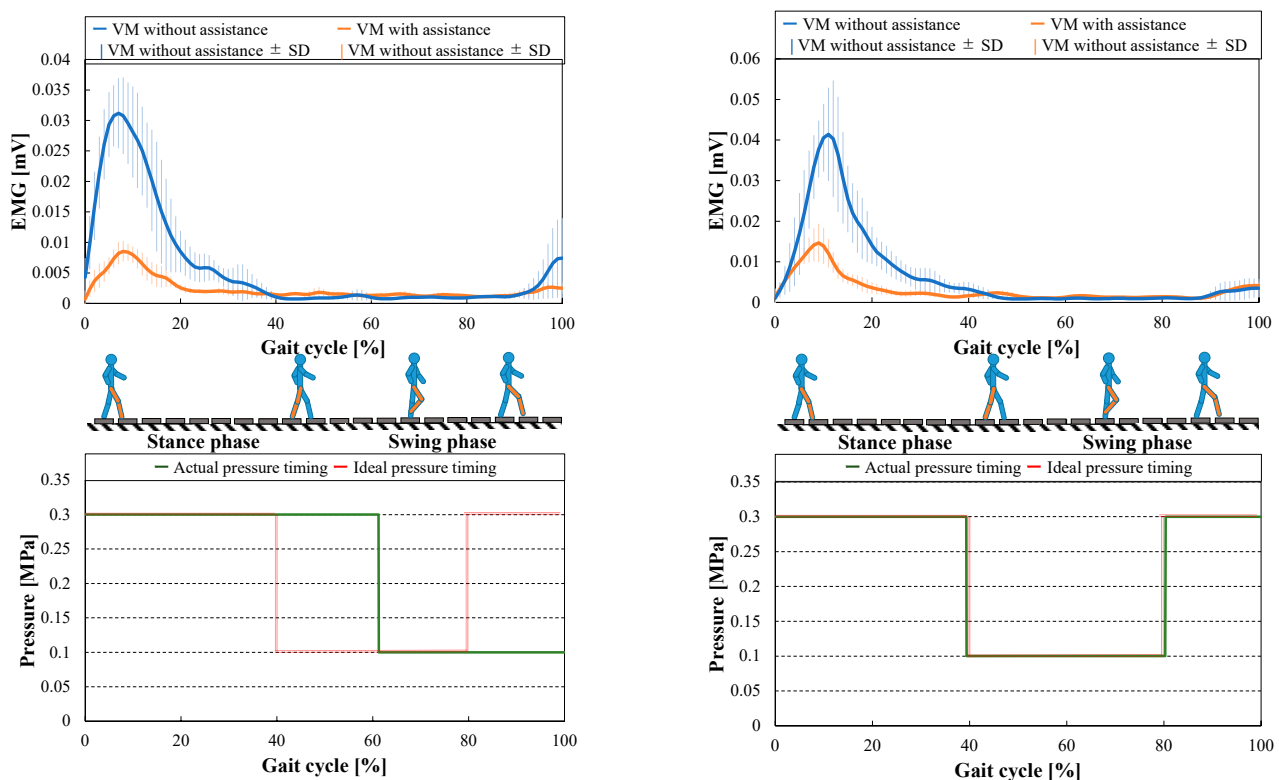
(**a**) VM of EMG and applied pressure in walking speed 3.0 km/h. (**b**) VM of EMG and applied pressure in walking speed 4.5 km/h.

Figure A1. Comparison of EMG with and without assistance and applied pressure to the prototype in one gait cycle (3.0 km/h and 4.5 km/h).

References

1. Evans, W. Functional and Metabolic Consequences of Sarcopenia. *J. Nutr.* **1997**, *127*, 988S–1003S.
2. Humphries, B.; McBride, T.T.; Newton, R.U.; Marshal, S.; Bronks, R.; McBride, J.; Hakkien, K.; Kraemer, W.J. The Relationship Between Dynamic, Isokinetic and Isometric Strength and Bone Mineral Density in a Population of 45 to 65 Years Old Women. *J. Sci. Med. Sport* **1999**, *2*, 364–374. [CrossRef]
3. Goodpaster, B.H.; Carison, C.L.; Visser, M.; Kelly, D.E.; Scherzinger, A.; Harris, T.B.; Stamm, E.; Newman, A.B. Attenuation of skeletal muscle and strength in the elderly: The Health ABC Study. *J. Appl. Physiol.* **2001**, *90*, 2157–2165. [CrossRef] [PubMed]
4. Azegami, M.; Ohira, M.; Miyoshi, K.; Kobayashi, C.; Hongo, M.; Yanagihara, R.; Sadoyama, T. Effect of single and multi-joint lower extremity muscle strength on the functional capacity and ADL_IADL status in Japanese community-dwelling older adults. *Nurs. Health Sci.* **2007**, *9*, 168–176. [CrossRef] [PubMed]
5. Bize, R.; Johnson, J.A.; Plotnikoff, R.C. Physical activity level and health-related quality of life in the general adult population: A systematic review. *Prev. Med.* **2007**, *45*, 401–415. [CrossRef] [PubMed]
6. Hayashi, T.; Kawamoto, H.; Sankai, Y. Control Method of Robot Suit HAL working as Operator's Muscle using Biological and Dynamical Information. In Proceedings of the IEEE/RSJ International Conference on Intelligent Robots and Systems (IROS), Edmonton, AB, Canada, 2–6 August 2005; pp. 3063–3068.
7. Muramatsu, Y.; Umehara, H.; Kobayashi, H. Improvement and Quantitative Performance Estimation of the Back Support Muscle Suit. In Proceedings of the 35th International Conference of the IEEE Engineering Medicine and Biology Society (EMBS), Osaka, Japan, 3–7 July 2013; pp. 2844–2849.
8. Sasaki, D.; Noritsugu, T.; Takaiwa, M. Development of Pneumatic Lower Limb Power Assist Wear driven with Wearable Air Supply System. In Proceedings of the IEEE/RSJ International Conference on Intelligent Robots and Systems (IROS), Tokyo, Japan, 3–7 November 2013; pp. 4440–4445.
9. Okui, M.; Iikawa, S.; Yamada, Y.; Nakamura, T. Variable viscoelastic joint system and its application to exoskeleton. In Proceedings of the 2017 IEEE/RSJ International Conference on Intelligent Robots and Systems (IROS), Vancouver, BC, Canada, 24–28 September 2017; pp. 3897–3902.
10. ReWalk More Than Walking, ReWalk Robotics, Inc. Available online: http://rewalk.com/ (accessed on 1 March 2020).
11. ATOUN, ATOUN Inc. Available online: http://atoun.co.jp/ (accessed on 1 March 2020).
12. Hogan, N. Adaptive Control of Mechanical Impedance by Coactivation of Antagonist Muscles. *IEEE Trans. Autom. Control* **1984**, *AC-29*, 681–690. [CrossRef]

13. Sakaguchi, S.; Venture, G.; Coste, C.A.; Havashibe, M. Active joint viscoelasticity estimation of the human knee using FES. In Proceedings of the 4th IEEE RAS & EMBS International Conference on Biomedical Robotics and Biomechatronics, Rome, Italy, 24–27 June 2012; pp. 1644–1649.

14. Okui, M.; Iikawa, S.; Yamada, Y.; Nakamura, T. Fundamental characteristic of novel actuation system with variable viscoelastic joints and MR clutches for human assistance. *J. Intell. Mater. Syst. Struct.* **2017**, *29*, 1045389X1770521. [CrossRef]

15. Ivanenko, Y.P.; Poppele, R.E.; Lacquaniti, F. Five basic muscle activation patterns account for muscle activity during human locomotion. *J. Physiol.* **2004**, *556*, 267–282. [CrossRef] [PubMed]

16. Wada, T.; Sano, H.; Sekimoto, M. Analysis of Inertial Motion in Swing Phase of Human Gait and Its Application to Motion Generation of Transfemoral Prosthesis. In Proceedings of the IEEE/RSJ International Conference on Intelligent Robots and Systems (IROS), Chicago, IL, USA, 14–18 September 2014; pp. 2075–2080.

17. Ernesto, A.V.; Hugh, H. Agonist-antagonist active knee prosthesis: A preliminary study in level-ground walking. *J. Rehabil. Res. Dev.* **2009**, *46*, 361–373.

18. Kimura, S.; Suzuki, R.; Kashima, M.; Okui, M.; Nishihama, R.; Nakamura, T. Assistive method that controls joint stiffness and antagonized angle based on human joint stiffness characteristics and its application to an exoskeleton. In Proceedings of the 19th International Conference on Advanced Robotics (ICAR), Belo Horizonte, Brazil, 2–6 December 2019.

19. Kimura, S.; Suzuki, R.; Kashima, M.; Okui, M.; Nishihama, R.; Nakamura, T. Assistance by Controlling the Stiffness and Antagonized Angle of One side Spring Antagonized Joint and Application to Standing up and Gait motion. In Proceedings of the ROBOMECH 2019, Hiroshima, Japan, 5–8 June 2019.

20. Kimura, S.; Machida, K.; Suzuki, R.; Kashima, M.; Okui, M.; Nishihama, R.; Nakamura, T. Evaluation of basic characteristic of variable stiffness assist suit based on the one-sided spring antagonized joint. In Proceedings of the ROBOMECH 2020, Kanazawa, Japan, 27–30 May 2020.

21. Nakamura, T. Experimental Comparisons between McKibben type Artificial Muscles and Staraight Fiber Type Artificial Muscles. In Proceedings of the SPIE International Conference Smart Structures, Devices and Systems III, Adelaide, Australia, 10–13 December 2006; p. 641424.

22. Tomori, H.; Nakamura, T. Theoretical comparison of mckibben-type artificial muscle and novel straight-fiber-type artificial muscle. *Int. J. Autom. Technol.* **2011**, *5*, 544–550. [CrossRef]

23. Suzuki, R.; Okui, M.; Iikawa, S.; Yamada, Y.; Nakamura, T. Novel Feedforward Controller for Straight-Fiber-Type Artificial Muscle Based on an Experimental Identification Model. In Proceedings of the First IEEE-RAS International Conference on Soft Robotics (RoboSoft), Livorno, Italy, 24–28 April 2018; p. WeBT.3.

24. Hanten, W.P.; Schulthies, S.S. Exercise Effect on Electromyographic Activity of the Vastus Medialis Oblique and Vastus Lateralis Muscles. *Phys. Ther.* **1990**, *70*, 561–565. [CrossRef] [PubMed]

25. Takahashi, K.; Sato, Y.; Suzuki, M.; Murakami, K.; Onobe, J.; Fujisawa, H. Lower Limb Muscle Activities and Cardiopulmonary Function during Treadmill Walking with Partial Body Weight Support. *J. Phys. Ther. Sci.* **2011**, *26*, 83–88.

26. Oka, H.; Mori, E.; Kumamoto, M. Electromyographic Study of Lower Limb Muscle Activity Patterns During Normal Walking. *J. Kansai Med. Univ.* **1984**, *36*, 131–151. [CrossRef]

27. Kimura, S.; Suzuki, R.; Machida, K.; Nishihama, R.; Okui, M.; Nakamura, T. Proposal of Motion Judgment Algorithm Based on Joint Angle of Variable Elastic Assist Suit with High Back Drivability. *J. Robot. Mechatron.* **2020**, *32*, 863–875. [CrossRef]